Locations of Atmospheric Photoelectron Energy Peaks Relative to the Sun

R. A. Frahm, J. D. Winningham, J. R. Sharber,
Southwest Research Institute, 6220 Culebra Road, San Antonio, TX 78228, USA
M. W. Liemohn, Y. Ma,
Space Physics Research Laboratory, University of Michigan, 2455 Hayward Street, Ann Arbor, MI 48105, USA
A. J. Coates, D. R. Linder, Y. Soobiah,
Mullard Space Science Laboratory, University College London, London RH5 6NT, UK and the ASPERA-3 Team.
Swedish Institute of Space Physics, Box 812, Kiruna S-981, Sweden

Abstract

The solar photon spectrum contains both discrete spectral lines and continuua. These emissions interact with the Martian atmosphere, generating photoelectrons. One of the discrete lines generated by the Sun is the HeII emission at 30.4 nm, which ionizes carbon dioxide and atomic oxygen to form distinct electron peaks. Direct ionization produces electrons with an energy peak of about 27 eV while direct ionization coupled with molecular vibration and rotation produces electrons with energy peaks in the range of 21-24 eV.

At Mars, the photoelectron energy peaks are mainly generated near the exobase. Once photoionization occurs, the photoelectrons are confined to move along the local remanent magnetic field. Sometimes the direction of electron motion causes them to precipitate into the atmosphere; however, it is also probable that the photoelectrons are transported away from the planet.

Interactions of these electrons in the altitude range from just above the exobase to about three Mars radii (the Mars Express apoapsis) are infrequent, remaining intact until dispersed by interaction. Thus, the photoelectron energy peaks from HeII photoionization may be used as a tracer, providing important information on the morphology of the atmospherically generated photoelectron population. Example data from the ELectron Spectrometer (ELS) of the Analyzer of Space Plasmas and Energetic Atoms (ASPERA-3) experiment on the Mars Express (MEX) spacecraft show the robustness of these spectral tracers and emphasizes the role played by both the solar wind and the crustal magnetic field in determining the distribution of the photoelectron population in the Mars Environment.

Introduction

On June 3, 2003, the European Space Agency (ESA) launched the Mars Express (MEX) spacecraft. The MEX spacecraft reached Mars and was injected into orbit on December 25, 2003. An experiment on the MEX spacecraft is the Analyzer of Space Plasmas and Energetic Atoms-3 (ASPERA-3) [Barabash, *et al.*, 2004], which measures *in situ* ions, electrons, and energetic neutral atoms (ENAs) at Mars. The ASPERA-3 *in situ* electrons are measured by the Electron Spectrometer (ELS).

Prior to launch of the Mars Express spacecraft, it was known that the ionospheric electron spectrum contained photoelectron peaks from the photoionization of atmospheric gasses. These photoelectron peaks were most recently measured by the Electron Reflectometer (ER) [Mitchell *et al.*, 2001] flown on the Mars Global Surveyor (MGS). The major photoelectron peaks in the range of 21-24 eV and 27 eV result from photoionization by a solar He 30.4 nm photon of both carbon dioxide and atomic oxygen [Mantas and Hanson, 1979; Fox and Dalgarno, 1979]. The majority of these photoelectrons are generated near the Martian exobase (the point where the mean free path becomes equal to the scale height). Photoionization rates decrease throughout the exosphere as the density decreases for both carbon dioxide and atomic oxygen [Krasnopolsky and Gladstone, 1996]. The fractional contributor adding a minor amount of photoelectrons is mainly from atomic oxygen which occurs above 300 km. The majority of photoelectrons observed at higher altitudes arrive through transport from below [Mantas and Hanson, 1979].

Instrument

The ELS is a spherical tophat which samples electrons from a 4° thick measurement plane. The 360° measurement plane is divided into 16 sectors, each sector is 22.5° wide. ELS k-factor (average value is 7.23 ± 0.05 eV/volt) and resolution (average value is 0.083 ± 0.003 $\Delta E/E$) are slightly sector dependent and were determined by laboratory measurements at 10 keV. Energy deviations of the k-factor and resolution were folded into an energy-dependent relative microchannel plate (MCP) efficiency factor. This allowed determination of the energy independent physical geometric factor as 5.88×10^{-4} cm^2 sr.

ELS covers the energy range from 0.4 eV to 20 keV with two deflection power supplies. ELS deflection voltage ranges from 0 to 20.99 V for the low range and 0 to 2800.0 V for the high range (energy conversion is sector dependent, but approximately 150 eV and 20 keV for the maximum values). Each supply has a control resolution of 4096 linear voltage values within its full range. Of the 8192 possible deflection voltage values, 128 are selected to comprise the ELS energy sweep which occurs in 4 sec. The ELS energy sweep is a decay step sequence from its highest voltage to its lowest voltage. The last sweep step is used as a fly back step and ignored.

Most of the ELS data presented in this poster were acquired under normal energy resolution and high time resolution; however, some of the data was acquired in high energy resolution and high time resolution mode. In a few cases, data was used from ELS in its low energy resolution and low time resolution modes. High energy resolution means that energy steps are acquired less than ΔE apart and fully telemetered; in normal energy resolution, energy steps are acquired at ΔE apart and fully telemetered. In low energy resolution modes, data is acquired at energy steps which are ΔE apart, but degraded by addition (2, 4, or 8 energy steps) before being telemetered. In high time resolution, a complete ELS energy sweep occurs within 4 sec and fully telemetered. Lower time resolution modes are degraded by addition of full energy sweeps (2, 4, 8, or 16 sweeps) before being telemetered.

Observations

Mantas and Hanson [1979] showed cases of modeled atmospheric photoelectrons for both horizontal and vertical magnetic field conditions. Their calculations were made at altitudes below 300 km, where the bulk of the photoelectrons are produced. Their calculations suggest that the photoelectron flux would be transported along the magnetic field, which could reach nearly to infinity in the case of a vertical magnetic field, as long as there were no other influences on the electrons. ELS has indeed observed atmospheric photoelectrons at all measurement altitudes.

The peaks in the photoelectron region are a dominant feature which provide a unique signature of electrons which came from the atmosphere. Figure 1, shown in isometric configuration, presents a collection of electron energy spectra taken in a variety of Martian regions at various altitudes. The lowest altitude spectrum was obtained in the ionosphere near perigee (about 270 km in daylight) and the highest altitude spectrum was obtained near apogee (about 10,000 km in the Martian tail). The region of each spectrum which shows the photoelectron peaks is highlighted to indicate that this feature can be observed throughout the entire measurement altitude range. Figure 1 indicates that ELS observes the same electron peak feature as described by both Mantas and Hanson [1979] and Fox and Dalgarno [1979] at all measurement altitudes.

The calculations of Mantas and Hanson [1979] indicate that since the photoelectrons are trapped on magnetic field lines, we should expect that wherever atmospheric photoelectrons are observed, that is the magnetic field line that is/was connected to the source where these electrons were created. The solar wind influences the Martian magnetic field, causing bending, stretching, and perhaps, interconnection, particularly where the Martian field interfaces with the solar wind and the interplanetary magnetic field. This influence can be observed by estimating where atmospheric photoelectrons are observed in the Mars environment.

Figure 2 shows the results of a pilot study of the occurrence locations where atmospheric photoelectron peaks are observed by ELS. This figure covers roughly the time period from January 5, 2004 through November 12, 2004. Only data for ELS sector 3 is used in the pilot study where no attention was paid to the attitude of ELS sector 3. For reference, over plotted are the average positions of the Martian bow shock and magnetic pile-up boundary as specified by Vignes et al. [2000] using the MGS magnetometer. The Sun is to the right and the shape of the boundaries are determined by the solar wind flow.

In this figure, one observes that the frequency of atmospheric photoelectron peaks is largest on the dayside of the planet at low altitudes in the ionosphere where they are generated. Atmospheric photoelectrons are never observed in the solar wind. This is indicating that the solar wind is influencing the location of where the atmospheric photoelectron peaks are observed, by exerting a magnetohydrodynamic force that keeps these electrons confined.

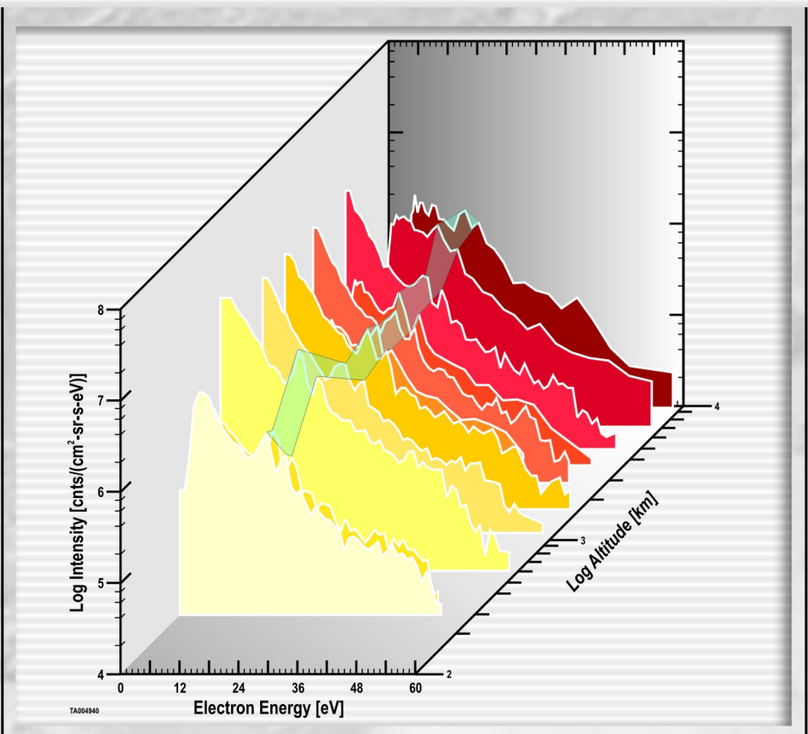

Figure 1. Altitudes where Atmospheric Photoelectron Peaks can be Observed. Presented are electron spectra obtained at perigee, apogee, and selected altitudes in between to show that the atmospheric photoelectron peaks can be found over the entire measurement range of the spacecraft. Location of the atmospheric photoelectron peaks are highlighted.

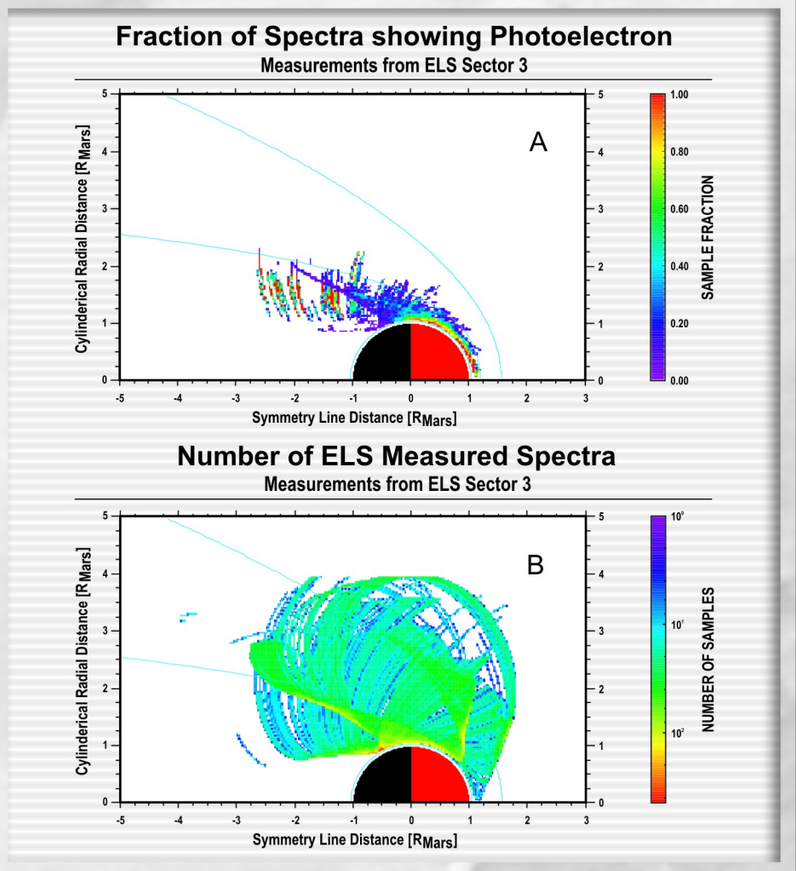

Figure 2. Fraction of Atmospheric Photoelectron Peaks. The region near Mars is examined to show the fractional of occurrence of atmospheric photoelectron peaks in (a) and number of samples made by the ELS in (b). In both cases, the sun is at the right and the average positions of the Martian bow shock and magnetic pile-up boundary as specified by Vignes *et al.* [2000] are shown.

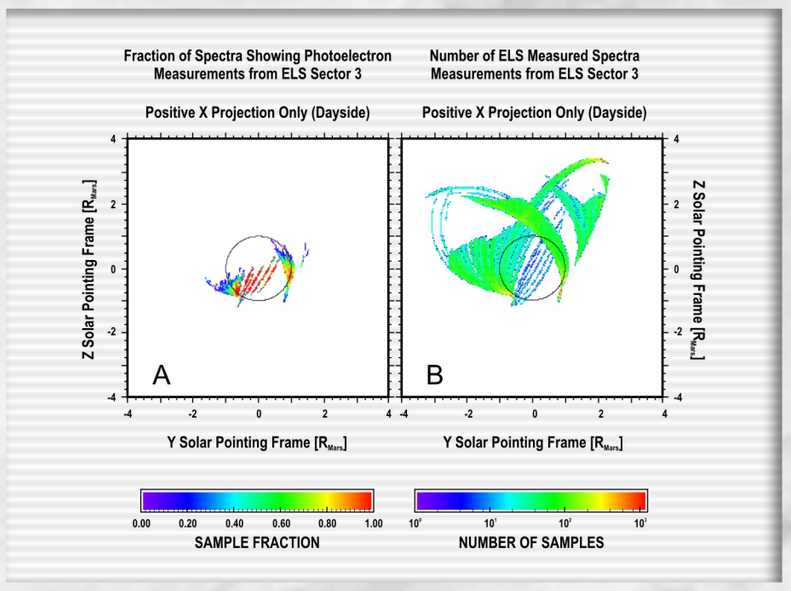

Figure 3. Dayside measurements projected into the Y-Z plane. The data shown in Figure 2 was resorted and shown on the Y-Z plane only for dayside data (X > 0), which show the location of measurements. The fraction of times photoelectrons are measured are shown in (a) while the total number of measurement points are shown in (b).

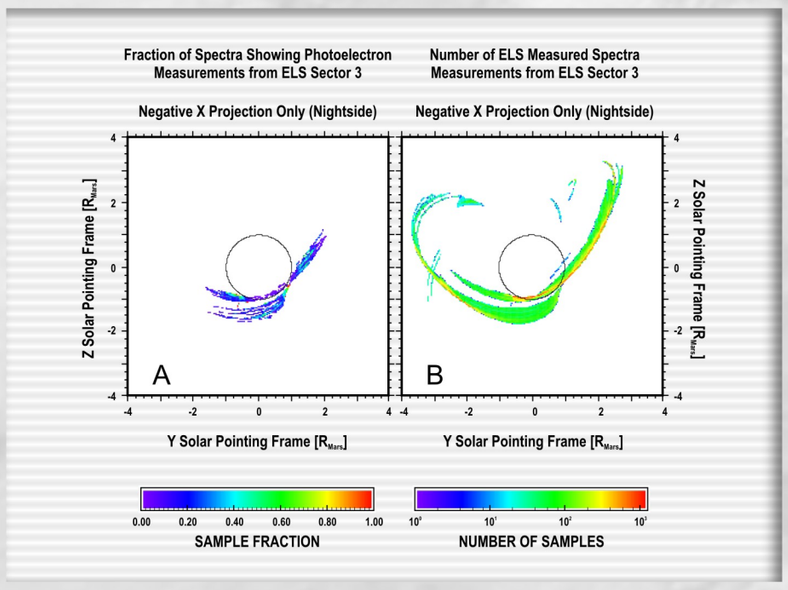

Figure 4. Nightside measurements projected into the Y-Z plane. The data shown in Figure 2 was resorted and shown on the Y-Z plane only for nightside data (X < 0), which show the location of measurements. The fraction of times photoelectrons are measured are shown in (a) while the total number of measurement points are shown in (b).

On the night side of the planet, atmospheric photoelectron peaks are never observed at high altitudes in the umbral region of the Martian tail; however, they are observed between the magnetic pile-up boundary and the umbral region. Near the planet on the night side, separated from the bulk of precipitation atmospheric photoelectron peaks are occasionally observed on magnetic field lines which map to production of atmospheric photoelectron peaks on the day side of the planet. This mapping suggests that some of the atmospheric photoelectrons which are created on the day side of the planet, travel down the tail near the magnetic pile-up boundary.

Since this data is expressed in coordinates relative to the Mars-Sun line, the data from Figure 2 are be resorted into projections on the Y-Z plane at X=0 for data on the day side of Mars (X > 0), shown in Figure 3, and data on the night side of Mars (X < 0). shown in Figure 4. These figures illustrate locations where ELS measurements were made and the subsequent bias in ELS coverage. Some details can be misleading, for example the lack of photoelectron measurements on the dayside of the planet in the north where there appear to be orbits (Figure 3b). At this location, MEX has gained too great of an altitude to measure atmospheric photoelectrons. There are some cases where this type of presentation is very useful. An example here is the group of photoelectrons detected on the night side of the planet just below the limb appear (in the south of Figure 4a) separated because the orbital trajectory does not measure continuously above the radial limb.

Discussion and Possible Scenarios

In the ionosphere, ELS measures the major photoelectron peaks created from photoionization of atmospheric gasses. Once liberated, the photoelectrons react to the environment in the same manner as any other electron. In general, electrons are organized by the magnetic field. The electrons travel adiabatically in the magnetic field until adiabatic conditions are violated and other forces in the magnetized fluid dominate. At this point, the electrons are no longer frozen to the magnetic field and their motion becomes flow dominated rather than magnetic field dominated.

There are several possibilities to explain how the atmospheric photoelectron peaks generated on the planet's dayside are found at 10,000 km in the tail. The first is that the electrons are tied to the field and they experience transport along that flux tube. In the front of the planet, the solar wind compresses the magnetic field and the shape of the field forms a closed loop with both feet of the field line attached to the planet. As the planet rotates toward the evening, magnetic field lines experience a change in the pressure direction and become stretched toward the tail (the field can be thought of as being dragged by the plasma flow in the magnetosheath). The observed electrons at 10,000 km could be contained on these closed field lines with one foot that is sunlit and generating atmospheric photoelectrons while the other foot is connected to a darkened ionosphere. Hence, flow should be observed in one direction. For both feet in a sunlit region, counter streaming flow should be observed. There are also possibilities of a kink, converging magnetic field line geometry, or scattering point along the magnetic field which could disrupt field aligned flow.

Another possibility is that the magnetic field has one foot connected to the planet while the other end of the field line connects to the magnetosheath or solar wind. Here, flow of sunlit atmospheric photoelectron peaks would be observed traveling away from the planet and only reflected toward the planet by a field line kink, converging magnetic field line geometry, or scattering point. This is in a sense, the vertical field of Mantas and Hanson [1979]. As a side note, if the field line is connected to both the planet and solar wind/magnetosheath, then it is likely that when atmospheric photoelectrons are observed flowing away from the planet, magnetosheath/solar wind electrons should be observed flowing toward the planet.

Yet another possibility is that the magnetic field lines on which sunlit atmospheric photoelectron peaks are observed in the tail consist of those which have been interconnected with the magnetosheath at the front of the magnetosphere. This innerconnection region could form a conduit for escape of atmospheric photoelectrons from the sunlit region. Basically, the region of interface between the magnetosheath and ionosphere could cause violation of adiabatic conditions such that atmospheric photoelectrons could travel through a region of confused magnetic field. As they are transported up along a field line connected to the sunlit atmosphere, they find themselves on a field line at the edge of the magnetosheath boundary as they travel through the region of confused magnetic field. The travel time for an electron generated in the sunlit hemisphere to be observed in the tail at 10,000 km is about 4-5 sec.

There is also a possibility that solar wind field lines intermix with chaotic crustal field lines at low altitudes such that the field lines from both sources become intertwined. Some of the atmospheric photoelectrons transfer to the solar wind magnetic field lines with little or no electron energization. These electrons flow down the solar wind field line which has propagated to the tail region of Mars.

Conclusion

Electrons liberated on the dayside of the planet from photoionization can be used as a tracer within the Martian Magnetosphere. It is observed that these electrons are confined to the dayside ionosphere and antisunward of the planet along and just inside the magnetic pile-up boundary defined from MGS magnetometer data. These electrons are not observed in the deep umbral tail. The location of photoelectrons in the Martian environment clearly reflects the influence of the solar wind on this population providing a means to study dayside to nightside transport of the photoelectrons and their relationship to the shocked solar wind population of the Martian magnetosphere.

Acknowledgements

The ASPERA-3 experiment on the European Space Agency (ESA) Mars Express mission is a joint effort between 15 laboratories in 10 countries, all sponsored by their national agencies. We thank all these agencies as well as the various departments/institutes hosting these efforts. We wish to acknowledge support through the National Aeronautics and Space Administration (NASA) contract NASW-00003 in the United States, Particle Physics and Astronomy Research Council (PPARC) in the United Kingdom, and wish to thank those NASA officials who had the foresight to allow augmentation of the original ASPERA-3 proposal for ELS so that it would provide the additional capabilities which allowed the science described in this paper to be conducted. We also wish to acknowledge the Swedish National Space Board for their support of the main PI-institute and we are indebted to ESA for their courage in embarking on the Mars Express program, the first ESA mission to the red planet.

References

Barabash, S., R. Lundin, H. Andersson, J. Gimholt, M. Holmström, O. Norberg, M. Yamauchi, K. Asamura, A. J. Coates, D. R. Linder, D. O. Kataria, C. C. Curtis, K. C. Hsieh, B. R. Sandel, A. Fedorov, A. Grigoriev, E. Budnik, M. Grande, M. Carter, D. H. Reading, H. Koskinen, E. Kallio, P. Riihela, T. Säles, J. Kozyra, N. Krupp, S. Livi, J. Woch, J. Luhmann, S. McKenna-Lawlor, S. Orsini, R. Cerulli-Irelli, A. Mura, A. Milillo, E. Roelof, D. Williams, J.-A. Sauvaud, J.-J. Thocaven, D. Winningham, R. Frahm, J. Scherrer, J. Sharber, P. Wurz, and P. Bochsler, "ASPERA-3: Analyser of Space Plasmas and Energetic Ions for the Mars Express," in *Mars Express: The Scientific Payload*, eds. A. Wilson and A. Chicarro, European Space Agency Special Report SP-1240, European Space Agency Research and Scientific Support, European Space Research and Technology Centre, Noordwijk, The Netherlands, 121-139, August 2004.

Fox, J. L., and A. Dalgarno, "Ionization, Luminosity, and Heating of the Upper Atmosphere of Mars," *Journal of Geophysical Research, 84*, 7315-7333, 1979.

Krasnopolsky, V. A., and G. R. Gladstone, "Helium on Mars: EUVE and PHOBOS data and implications for Mars' evolution," *Journal of Geophysical Research, 101*, 15765-15772, 1996.

Liemohn, M. W., *et al.*, "Numerical interpretation of high-altitude photoelectron observations," *Icarus*, in press, 2006.

Mantas, G. P., and W. B. Hanson, "Photoelectron Fluxes in the Martian Ionosphere," *Journal of Geophysical Research, 84*, 369-385, 1979.

Mitchell, D. L., R. P. Lin, C. Mazelle, H. Rème, P. A. Cloutier, J. E. P. Connerney, M. H. Acuña, and N. F. Ness, "Probing Mars' crustal magnetic field and ionosphere with the MGS Electron Reflectometer," *Journal of Geophysical Research, 106*, 23419-23427, 2001.

Vignes, D., C. Mazelle, H. Rème, M. H. Acuña, J. E. P. Connerney, R. P. Lin, D. L. Mitchell, P. Cloutier, D. H. Crider, and N. F. Ness, "The solar wind interaction with Mars: Locations and shapes of the bow shock and the magnetic pile-up boundary from the observations of the MAG/ER experiment onboard Mars Global Surveyor," *Geophysical Research Letters, 27*, 49-52, 2000.

ASPERA-3 Team

R. A. Frahm, J. D. Winningham, J. R. Sharber, SwRI, San Antonio, USA
A. J. Coates, D. R. Linder, D. O. Kataria, Mullard Space Science Laboratory, UCL, UK
R. Lundin, H. Anderson, S. Barabash, M. Holmström, M. Yamauchi, Swedish Institute of Space Physics, Sweden
E. Kallio, H. Koskinen, Finnish Meteorological Institute, Helsinki, Finland
J. Kozyra, Space Physics Research Laboratory, U. Michigan, Ann Arbor, USA
J. Luhmann, University of California Berkeley, USA
E. Roelof, D. Williams, JHU-APL, Laurel, USA
C.C. Curtis, K. C. Hsieh, B. R. Sandel, University of Arizona, Tucson, USA
J. A. Sauvaud, A. Federov, Centre d'Etude Spatiale des Rayonnements, France
S. McKenna-Lawlor, Space Technology Ltd, Maynooth, Ireland
S. Orsini, R. Cerulli-Irelli, Institute di Fisica dello Spazio Interplantari, Italy
P. Bochsler, P. Wurz, University of Bern, Bern Switzerland
K. Azamura, ISAS, Japan
M. Grande, Rutherford Appleton Laboratory, Oxfordshire, UK
N. Krupp, J. Woch, M. Fraenz, Max-Planck-Institut fur Aeronomie, Germany